JOC Article

Photophysics and Photochemistry of Naphthoxazinone Derivatives

Santi Nonell,[†] Lourdes R. Ferreras,[†] Alvaro Cañete,[‡] Else Lemp,[‡] German Günther,[‡] Nancy Pizarro,[‡] and Antonio L. Zanocco*,[‡]

Grup d'Enginyeria Molecular, Institut Químic de Sarrià, Universitat Ramon Llull, Via Augusta 390, E-08017, Barcelona, España, and Facultad de Ciencias Químicas y Farmacéuticas, Departamento de Química Orgánica y Fisicoquímica, Universidad de Chile, Casilla 233, Santiago - 1, Santiago, Chile

azanocco@ciq.uchile.cl

Received January 17, 2008

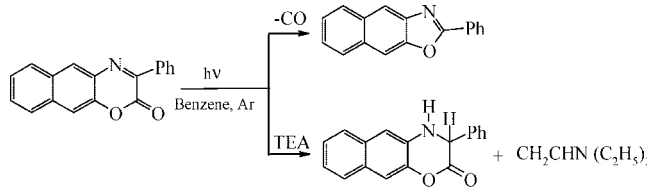

The photophysics and photochemistry of a series of naphthoxazinones have been studied using a combination of methods ranging from steady-state and time-resolved spectroscopic techniques to product analysis. The photophysics of naphthoxazinone derivatives is very dependent on the structure: phenanthrene-like compounds exhibit higher fluorescence quantum yield than the less aromatic anthracene-like homologous. The latter, exhibit a substantial degree of charge transfer in the excited singlet state. These compounds are fairly photostable in the absence of additives, yielding a single photoproduct arising from the triplet state. The presence of electron donors such as amines increases the photoconsumption quantum yield and changes the product distribution, the primary photoproduct being a dihydronaphthoxazinone that photoreacts further yielding ultimately an oxazoline derivative.

Introduction

Benzoxazinone derivatives are a class of compounds exhibiting spectral and photophysical properties of great interest such as broad first absorption band, emission in the red, intense fluorescence in both organic solutions and crystalline state, large dipole moment increase in the excited state, large Stokes shifts, and short fluorescence lifetimes.[1–4] Regarding these properties, it has been suggested that this type of compounds can be employed as quantum counters, wavelength shifters, fluorescent solar concentrators, fluorescent probes for biological systems, and laser dyes.[5–13] In spite of this interest, few studies addressing the photochemistry of aryloxazinones have been carried out. Light induced reactions of 1,4-benzoxazin-2-ones with electron-deficient olefins have been described by Nishio et al.[14,15] Irradiation of a mixture of 3-methyl-1,4-benzoxazin-2-one and an excess of methacrylonitrile under nitrogen atmosphere gave two stereoisomeric azetidine derivatives. In the presence of an excess methyl methacrylate also two stereoisomeric photocycloadducts were formed (Scheme 1). Formation of the photocycloadducts was completely quenched by oxygen and *trans*-stilbene suggesting a reaction involving the triplet excited state. No cycloadduct formation was observed when the methyl substituent of the benzoxazinone was replaced with a phenyl

* To whom correspondence should be addressed. Phone: 56-2-6782877. Fax: 56-2-6782868.
[†] Universitat Ramon Llull.
[‡] Universidad de Chile.

(1) Le Bris, M. T. *J. Heterocyclic Chem.* **1984**, *21*, 551–555.
(2) Le Bris, M. T. *J. Heterocyclic Chem.* **1985**, *22*, 1275–1280.
(3) Le Bris, M. T.; Mugnier, J.; Boursons, J.; Valeur, B. *Chem. Phys. Lett.* **1985**, *1*, 124–127.
(4) Le Bris, M. T. *J. Heterocyclic Chem.* **1989**, *26*, 429–433.
(5) Dupuy, F.; Rullière, C.; Le Bris, M. T.; Valeur, B. *Opt. Commun.* **1984**, *51*, 36–40.
(6) Mugnier, J.; Dordet, Y.; Pouget, J.; Le Bris, M. T.; Valeur, B. *Sol. Energy Mater.* **1987**, *15*, 65–75.
(7) Monsigny, M.; Midoux, P.; Le Bris, M. T.; Roche, A. C.; Valeur, B. *Biol. Cell* **1989**, *67*, 193–200.
(8) Monsigny, M.; Midoux, P.; Depierreux, C.; Bebear, C.; Le Bris, M. T.; Valeur, B. *Biol. Cell* **1990**, *70*, 101–105.
(9) Depierreux, C.; Le Bris, M. T.; Michel, M. F.; Valeur, B.; Monsigny, M.; Delmotte, F. *FEMS Microbiol. Lett.* **1990**, *67*, 237–243.
(10) Fery-Forgues, S.; Le Bris, M. T.; Guette, J. P.; Valeur, B. *J. Phys. Chem.* **1988**, *92*, 6233–6237.
(11) Fery-Forgues, S.; Le Bris, M. T.; Guette, J. P.; Valeur, B. *J. Chem. Soc., Chem. Commun.* **1988**, *5*, 384–385.
(12) Khochkina, O. I.; Sokolova, I. V.; Loboda, L. I. *Russ. Phys. J.* **1988**, *31*, 510–513.
(13) Fery-Forgues, S.; Le Bris, M. T.; Mialocq, J.-C.; Pouget, J.; Rettig, W.; Valeur, B. *J. Phys. Chem.* **1992**, *96*, 701–710.
(14) Nishio, T.; Omote, Y. *J. Org. Chem.* **1985**, *50*, 1370–1373.
(15) Nishio, T. *J. Chem. Soc., Perkin Trans. I* **1990**, 565–570.

10.1021/jo800039r CCC: $40.75
Published on Web 06/14/2008

SCHEME 1

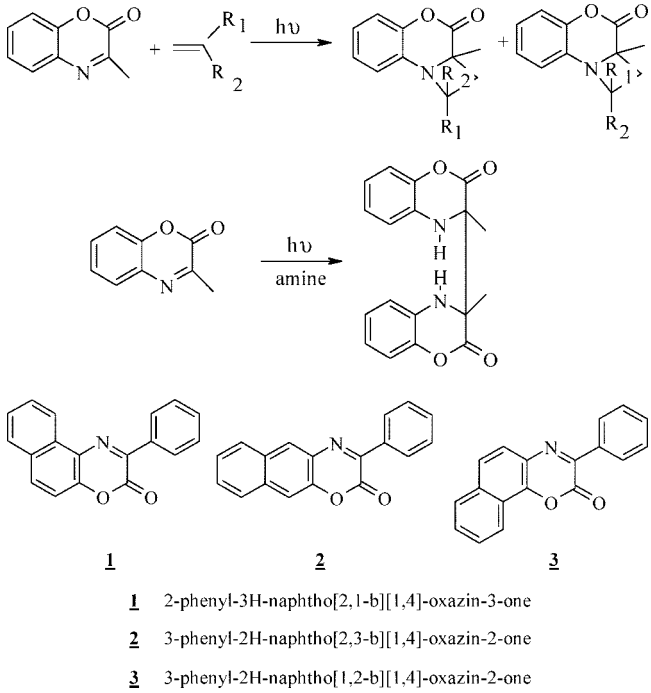

FIGURE 1. Chemical structures of the studied naphthoxazinones.

group and when the photolysis was conducted in the presence of amines such as triethylamine. In the last case the main photoreaction products are reductive dimers in moderate yields (Scheme 1). A reaction mechanism involving the formation of an exciplex between the oxazinone triplet and the olefin was proposed, whereby the exciplex evolves to a 1,4-birradical intermediate which ultimately leads to the observed products.[14] In the presence of amines, electron transfer from the amine to the benzoxazinone triplet and subsequent hydrogen abstraction leading to the products has been suggested as the reaction mechanism.

Building on the fact that the benzoxazinone excited states have substantial charge-transfer character, we hypothesized that substitution of the benzo- with a naphtho-group could substantially affect the photophysical and photochemical properties of the aryloxazinones. In this work, we report on the synthesis and photochemistry of three naphthoxazinone derivatives (Figure 1). These compounds all contain a phenyl group at the carbonyl's α position, which should prevent the formation of cyclic photoproducts, and differ in the position where the oxazinone ring is fused to the naphtho group and in their relative orientation, resulting in significant changes in their photophysical properties. The properties evaluated for these compounds suggest that they are valuable candidates for technological applications, such as dyes, quantum counters, or fluorescent probes.

Results and Discussion

Absorption and Fluorescence Spectra. The absorption spectra of compounds **1**−**3** are nearly independent of solvent polarity. Compound **2** exhibits the maximum of the lowest-energy absorption band (λ_{max}^{Abs}) centered around 350 nm whereas for compounds **1** and **3** the maxima appear between 392 and 398 nm. Spectra calculations employing DFT formalism (B3LYP-6311 g+ for structure optimization and ZINDO-S to calculate

TABLE 1. Solvent Dependence of the Absorption and Fluorescence Transitions

	λ_{max}^{Abs} (ε)/λ_{max}^{Em} [a]		
	1	**2**	**3**
hexane	392 (19140)/453	350 (23290)/500, 483	398 (12110)/459
benzene	398 (19020)/467	356 (23150)/514	396 (12370)/478
acetonitrile	392 (18820)/475	348 (24140)/538	396 (11270)/490
methanol	394(18650)/476	346 (23630)/548	396 (11045)/511

[a] λ_{max}^{Abs}, λ_{max}^{Em} in nm; ε in M^{-1} cm^{-1}

the Franck−Condon transitions) overestimate λ_{max} by about of 20 nm, however analysis of molecular orbital indicates a π-π^* transition in all cases. The results are comparable to those reported for benzoxazinone derivatives[2] and structurally related compounds such as coumarins.[16] Values of λ_{max}^{Abs} and molar absorption coefficient are collected in Table 1. The polarity of the solvent has a large effect on the fluorescence spectrum of compounds **1** − **3**. The red shift is quite large in polar solvents: for compound **2**, the position of the emission maximum (λ_{max}^{Em}) shifts from 500 nm in *n*-hexane to 548 nm in methanol, while for compound **3** λ_{max}^{Em} shifts from 459 nm in *n*-heptane to 506 nm in ethylene glycol. Representative values of λ_{max}^{Em} in selected solvents are collected in Table 1.

These shifts can be analyzed in terms of various solvatochromic scales. We have chosen the LSER equation (eq 1) introduced by Kamlet et al.:[17,18]

$$P = P_0 + a\pi^* + b\alpha + c\beta + d\rho_H^2 \qquad (1)$$

where P is an energy-dependent property, π^* accounts for dipolarities and polarizabilities of solvent, α is related to the hydrogen bond donor solvent ability, β indicates the solvent capacity as hydrogen bond acceptor, and ρ_H^2 is the square of Hildebrand parameter, which accounts for the solvent cohesive energy density and models the cavity effects.[17,19,20] Compared to other empirical scales such as $E_T(30)$,[21] equation 1 was established studying the behavior of many different chromophores and therefore offers the advantage of its wider applicability. Also, it enables the separation of specific hydrogen-bonding effects.

The studied naphthoxazinone derivatives are not hydrogen-bond donors but only hydrogen-bond acceptors mainly on the carbonyl and the imino groups; hence, the dependence of λ_{max}^{Em} on solvent is expected to involve only two parameters, the dipolarity/polarizability π^* and the hydrogen-bonding ability α.[17] Indeed, the results of multilinear regression analysis by employing StatView 5.0 statistical software confirm that the values of λ_{max}^{Em} depend only on the microscopic solvent parameters π^* and α, showing red-shifts in solvents able to stabilize charges and dipoles as well as in solvents with high α values (Table 2).

Correlation equations result from purely statistical criteria. The overall correlation equation quality is indicated by the sample size, N, the product correlation coefficient, R, and the

(16) Kovac, B.; Novak, I. *Spectrochim. Acta* **2002**, *58*, 1483–1488.
(17) Taft, R.W.;; Kamlet, M. J. *J. Am. Chem. Soc.* **1976**, *98*, 2886–2894.
(18) Kamlet, M. J.; Hall, T. N.; Boykin, J.; Taft, R. W. *J. Org. Chem.* **1979**, *44*, 2599–2604.
(19) Kamlet, M. J.; Abboud, J. L. M.; Abraham, M. H.; Taft, R. W. *J. Am. Chem. Soc.* **1977**, *99*, 6027–6038.
(20) Kamlet, M. J.; Abboud, J. L. M.; Abraham, M. H.; Taft, R. W. *J. Org. Chem.* **1983**, *48*, 2877–2887.
(21) Reichardt, C. *Solvents and Solvent Effects in Organic Chemistry*, 3rd ed.; WILEY-VCH: Weinheim, 2003.

TABLE 2. LSER Correlation Equations ($\bar{\nu} = \bar{\nu} + a\pi^* + b\alpha + c\beta + d\rho_H^2$) for the Dependence of the λ_{max}^{Em} (Expressed in cm^{-1}) on the Solvent Parameters

	$\bar{\nu}_0$	*a*	*b*
	1		
Coeff	21951.4	−1079.9	−266.0
±	42.6	69.9	53.3
t-stat	517.0	−15.5	−4.9
P(2-tail)	<0.0001	<0.0001	0.0008
	$N = 12$	$R = 0.99$	$F = 181.4$
	2		
Coeff	20220.7	−1667.1	−1016.4
±	211.4	319.1	166.8
t-stat	95.6	−5.2	−6.1
P(2-tail)	<0.0001	0.0003	<0.0001
	$N = 14$	$R = 0.91$	$F = 26.7$
	3		
Coeff	21627.9	−1452.3	−641.6
±	76.7	114.5	77.2
t-stat	281.9	−12.7	−8.3
P(2-tail)	<0.0001	<0.0001	<0.0001
	$N = 17$	$R = 0.97$	$F = 120.5$

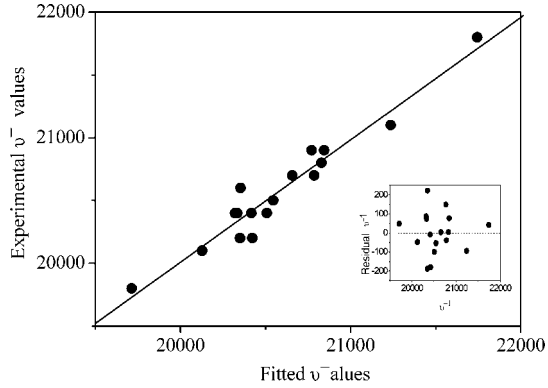

FIGURE 2. Plot of $\bar{\nu}$ (exp) vs $\bar{\nu}$ (calc) for the dependence of the λ_{max}^{Em} on the solvent for compound **3**. (Inset) Plot of the residuals of $\bar{\nu}$ vs $\bar{\nu}$.

Fisher index of equation reliability, *F*. The consistency of each term is indicated by the standard error, ±, the 2-tail probability, P(2-tail), and the *t*-statistic. Good quality is indicated by higher *F* and *t*-stat values, and by small SD ones. Descriptor coefficients accepted in the correlation equation were those that had a significance level ≥ 0.95. As anticipated, all compounds show a similar behavior. Figure 2 shows a plot of the experimental vs calculated λ_{max}^{Em} (expressed in wavenumbers) for the naphthoxazinone **3** computed according to the LSER equation in Table 1.

The good agreement between the two sets of data confirms the importance of π^* and α in the solvent dependence of the λ_{max}^{Em} values. The plot of residuals in the inset of Figure 2 shows a random distribution of residuals in the range of λ_{max}^{Em} values. These results are strong evidence that a substantial charge-separation occurs in the first excited singlet state.

The red-shift can be interpreted in terms of an increased dipole moment of the naphthoxazinones upon chromophore excitation and subsequent solvent relaxation. Indeed a Lippert−Mataga plot[22,23] of the Stokes shift vs the solvent polarity function yields the difference of dipole moments between the excited- and ground states ($\mu^* - \mu^0$). The results collected in Table 3 were obtained employing values of the Onsager cavity radius calculated from the minimized structures (B3LYP-6311 g+) under Gaussian 03 environment.

TABLE 3. Difference of Dipole Moments between the Excited- and Ground States of Compounds 1, 2, and 3

compound	Onsager radius/Å[a]	$\mu^* - \mu^0$/Debye
1	4.9	6.1
2	5.1	11.1
3	4.9	7.9

[a] Calculated using computational methods.

The dipole moment differences between the S_1 and S_0 states are similar for compounds **1** and **3** and substantially larger for compound **2**. The results are comparable to those determined for coumarin derivatives,[24] though smaller than those reported for styryl derivatives of aminobenzoxazinones.[13] Mulliken charge analyses show charge separation mainly involving atoms in the oxazinone ring with the dipole in the molecular plane oriented close to the carbonyl bond axis. The dependence of the fluorescence spectrum on the solvent parameters π^* and α and the large increase in dipole moment upon excitation suggest an substantial charge-transfer character of the first excited singlet state, particularly for compound **2**.

Fluorescence Quantum Yield and Lifetime. The fluorescence quantum yields, Φ_F, of compounds **1** and **3** are high and similar in polar solvents, decreasing to different extents as the solvent polarity is lowered (Table 4). In contrast, compound **2** has a very low fluorescence quantum yield, close to the detection limit of our measurement system. This is consistent with its higher triplet yield (*vide infra*) and is related to structural and energetic factors that contribute to the molecule aromaticity (benzoannelation phenomena).[25,26] Values of the fluorescence lifetime in benzene, measured by employing the phase demodulation method, are likewise collected in Table 4. Naphthoxazinones **1** and **3** are compounds with phenanthrene-like structure whereas naphthoxazinone **2** has an anthracene-like geometry. Fluorescence data indicates that the inclusion of the heterocyclic ring produces substantial differences when the same parameters for the aromatic compounds, anthracene and phenanthrene, are considered. Anthracene fluorescence lifetime and fluorescence quantum yield are a factor twelve and a factor two larger than those reported for phenanthrene, respectively,[27] being the first one more aromatic than the angular catacondensed homologous.[26] Various studies indicate that a highly fluorescent molecule must have rigid structure with an extensive delocalized π double bond system, because $\pi-\pi^*$ transitions possess high values of the molar absorbility coefficient and low decay half-times other processes such as intersystem crossing cannot compete with the fluorescence.[28,29] These features are accomplished by aromatic molecules so that the vast majority of luminophores are aromatic. Furthermore, from semiempirical calculations has been suggested that, in coumarins, quinoxalinones, and benzoxazinones, the intersystem crossing from the

(22) Lippert, E. *Z. Naturforsch.* **1955**, *10*, 541–547.
(23) Mataga, N.; Chosrowjan, H.; Taniguchi, S. *J. Photochem. Photobiol. C: Photochem. Rev.* **2005**, *6*, 37–79.
(24) Cave, R. J.; Castner, E. W. *J. Phys. Chem. A* **2002**, *106*, 12117–12123.
(25) Krygowski, T. M.; Cyranski, M. *Tetrahedron* **1996**, *52*, 13795–13802.
(26) Krygowski, T. M.; Cyranski, M. K. *Chem. Rev.* **2001**, *101*, 1385–1419.
(27) Dabestani, R.; Ivanov, I. N. *Photochem. Photobiol.* **1999**, *70*, 10–34.
(28) Nijegorodov, N.; Winkoun, D. P. *Spectrochim. Acta* **1997**, *53*, 2013–2022, Part A
(29) Gikas, E.; Parissi-Poulou, M.; Kazanis, M.; Vavagiannis, A. *J. Mol. Struct.: Theochem.* **2005**, *724*, 135–142.

TABLE 4. Summary of Photophysical Parameters for the Singlet Excited States

	Φ_F				K_{SV}^{TEA}/M^{-1}	τ_S^0/ns	$^1k_q^{TEA}/10^{10}$ $M^{-1}s^{-1}$
compound	hexane	benzene	CH_3CN	CH_3OH	benzene		
1	0.12	0.46	0.56	0.50	27.3	2.2	1.2
2	<0.003	<0.003	<0.003	<0.003	15.7	1.2	1.3
3	0.32	0.46	0.50	0.45	40.1	6.0	0.7

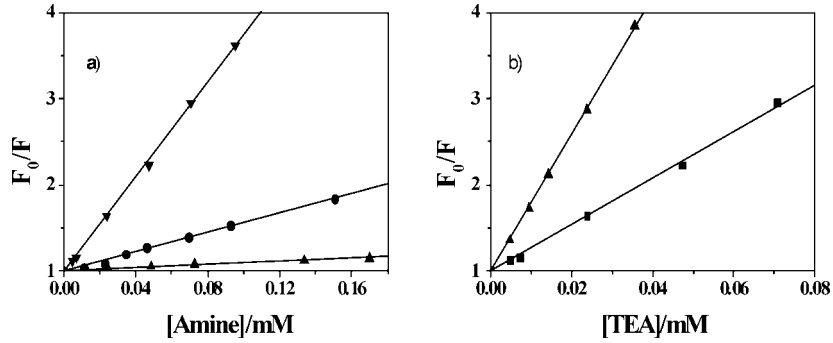

FIGURE 3. (a) Dependence of the fluorescence quenching of naphthoxazinone **1** on the amine ionization potential in benzene as solvent: ▼ triethylamine, ● diethylamine, ▲ *n*-butylamine. (b) Dependence of the fluorescence quenching of naphthoxazinone **1** by triethylamine on the solvent: ▲ acetonitrile, ■ benzene.

$S_1(\pi,\pi^*)$ state to the $T_n(n,\pi^*)$ state competes with the fluorescence, and their Φ_F values can be predicted by calculating the $\Delta E(T_n(n,\pi^*),S_1(\pi,\pi^*))$ values (the energy gap between the $T_n(n,\pi^*)$ and $S_1(\pi,\pi^*)$ states). The compounds having a higher $T_n(n,\pi^*)$ state (the lowest triplet n,π^* state) than the $S_1(\pi,\pi^*)$ state (the fluorescent state) strongly fluoresce.[29]

Naphthoxazinone derivatives show an opposite trend than that observed for aromatic hydrocarbons such as anthracene and phenantrene, being larger the fluorescence quantum yield and the fluorescence lifetime for the phenanthrene-like compounds than those determined for the anthracene-like oxazinones. These differences could be ascribed to the effect of the heterocyclic ring on the system aromaticity and the triplet excited states manifold. The B3LYP-6311g+ calculations show that compounds **1** and **3** have extensive delocalization of molecular orbitals HOMO and LUMO involving the naphthalene moiety, the oxazinone ring and the phenyl substituent. For compound **2**, it was found that the HOMO is mainly localized on the oxazinone ring and the neighbor condensed aromatic ring whereas the phenyl substituent practically does not contribute to the HOMO delocalization. Consequently, from the aromaticity point of view, compounds **1** and **3** would be more fluorescent than **2**. In addition, within the limitations of ZINDO calculations conducted in vacuo, for the naphthoxazinone derivative **2**, it was found that the energies of the higher $T_n(n,\pi^*)$ states (T_4, T_5, and T_6) are lower than the energy of the $S_1(\pi,\pi^*)$ state, whereas for compounds **1** and **3**, T_3 is the lower triplet whose energy is near to the $S_1(\pi,\pi^*)$ state. Considering the larger spin−orbit coupling for $S_1(\pi,\pi^*) \rightarrow T_n(n,\pi^*)$ transitions, the El-Sayed rules[30,31] and Salem propositions,[32,33] an efficient intersystem crossing process can be expected for compound **2** concomitant with the very low fluorescence quantum yield experimentally observed.

Fluorescence Quenching by Amines. The fluorescence is quenched by adding increasing amounts of various amines to the solutions. Typical Stern-Volmer plots for naphthoxazinone **1** obtained under several experimental conditions are shown in Figure 3. The plots were linear in the quencher concentration range assayed. Table 4 also gives the values of the bimolecular rate constant for singlet quenching, $^1k_q^{TEA}$, calculated as $^1k_q^{TEA} = K_{SV}^{TEA}/\tau^0_S$. They are close to the diffusion control limit for all compounds and is ca. 2-fold larger in acetonitrile relative to benzene (Figure 3b) reflecting the higher diffusional limit in acetonitrile. The Stern−Volmer constants K_{SV} obtained from the slope of plots of Figure 3a give a good lineal correlation with the amine ionization potential, increasing as the ionization potential of the amine decreases. This result would be indicative of the electron-transfer mechanism for quenching of naphthoxazinone derivatives by amines.

Phosphorescence Spectra and Triplet Energy. Emission spectra were recorded in both methyltetrahydrofuran (MTHF) and in methyl cyclohexane/1,2-diiodoethane (4:3) at 77 K. Phosphorescence could only be observed in the heavy-atom containing solvent and only for **2**. From the onset of the phosphorescence at ca. 640 nm, we estimate the triplet energy level of **2** at 188 ± 5 kJ·mol^{-1} (Figure 4).

Triplet Absorption Spectra and Lifetime. Nanosecond-laser flash excitation of argon-saturated benzene solutions of the compounds resulted in transient absorbance changes, which could be quenched by oxygen and thus were attributed to their triplet state. The differential triplet-minus-singlet absorption spectra are shown in Figure 5. The lifetime values are collected in Table 5. Similarly as found for the singlet state, naphthoxazinone **3** has also a remarkably longer triplet lifetime than the other two compounds examined.

Singlet Oxygen Photosensitization. The triplet lifetime decreases significantly in the presence of oxygen (Table 2), indicating efficient energy transfer to this molecule. Using time-resolved singlet oxygen $O_2(^1\Delta_g)$ phosphorescence detection at 1270 nm, the quantum yield of $O_2(^1\Delta_g)$ production, Φ_Δ, has been readily determined. The values for the three compounds are collected in Table 5 and are consistent with the fluorescence quantum yields, that is, Φ_Δ is highest for the nonfluorescent compound **2**, indicating that intersystem-crossing is a major

(30) El-Sayed, M. A. *J. Chem. Phys.* **1963**, *38*, 2834–2838.
(31) El-Sayed, M. A. *J. Chem. Phys.* **1964**, *41*, 2462–2467.
(32) Salem, L.; Rowland, C. *Angew. Chem., Int. Ed. Engl.* **1972**, *11*, 92–111.
(33) Salem, L. *Pure Appl. Chem.* **1973**, *33*, 317–328.

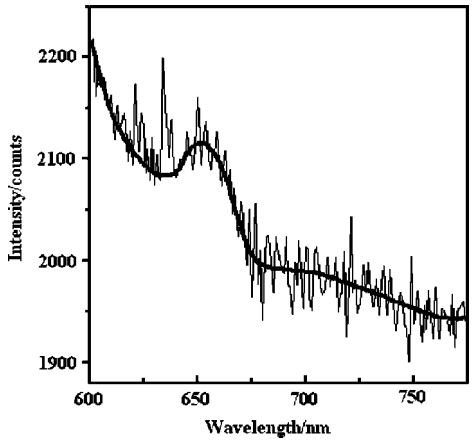

FIGURE 4. Emission spectrum of **2** in methyl cyclohexane/1,2-diiodoethane (4:3) at 77 K.

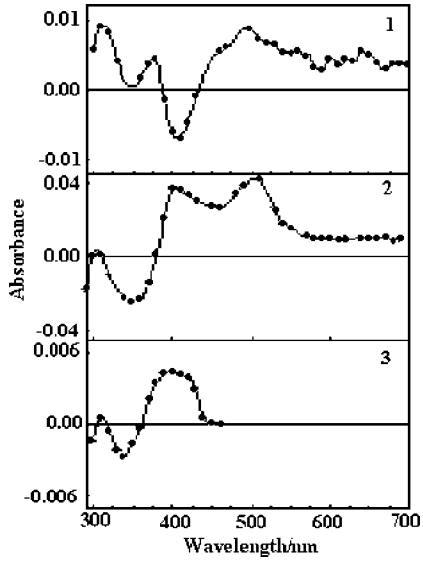

FIGURE 5. Transient absorption spectrum at 1 μs delay alter laser flash excitation of Ar-saturated benzene solutions of **1**, **2**, and **3**.

TABLE 5. Summary of Photophysical Parameters for the Triplet State in Benzene

	lifetime (Ar)/ μs	lifetime (air)/ μs	$^3k_q^{TEA}/10^5$ M^{-1} s^{-1}	Φ_Δ
1	31	0.39	1.3 ± 0.1	0.26 ± 0.01
2	36	0.24	3.1 ± 0.1	0.48 ± 0.03
3	60	0.30	1.5 ± 0.1	0.15 ± 0.01

deactivation pathway for this naphthoxazinone. We also measured the compounds ability to quench singlet oxygen and found it to be negligible, with rate constants $^\Delta k_q < 10^5$ $M^{-1}s^{-1}$ for **1** and **3**, and $^\Delta k_q < 10^4$ $M^{-1}s^{-1}$ for **2**.

Rate Constants for Triplet Quenching by TEA. Addition of increasing amounts of TEA to Ar-saturated benzene solutions of the compounds resulted in a concomitant increase in the decay rate of their triple state. Analysis of Stern-Volmer plots using $^3k_{obs} = 1/\tau_T = 1/\tau^0_T + {}^3k_q^{TEA}[TEA]$ yielded the quenching rate constants collected in Table 5, with compound **2** ca. twice as reactive as compounds **1** and **3**. The rate constants for quenching of the triplet state are five orders of magnitude smaller than those for the singlet state. A clear decrease in the *amplitude* of the transients could also be observed, consistent with the quenching of the singlet state precursor by TEA (see above).

Photochemical Reactions. Irradiation of compounds **1**−**3** (λ = 366 nm) under Ar in benzene lead to a decrease in the concentration of the naphthoxazinones. No consumption was observed when the same experiment was carried out in O_2-purged solutions. In the presence of TEA, the rate of naphthoxazinone-derivative consumption increased in a TEA-concentration dependent way. The photoconsumption quantum yields were extrapolated to zero irradiation time and measured under several experimental conditions. The self-sensitized photoxygenation of 9,10-dimethylanthracene was used as actinometer.

Product distribution of naphthoxazinone **1** photoreaction in benzene, was analyzed by obtaining GC-MS chromatograms before and after exhaustive photolysis of compound **1** under Ar. The time zero chromatogram shows a single peak at 15.94 min, corresponding to naphthoxazinone **1** as verified by its mass spectra. The photolyzed solution shows a single additional peak at 13.22 min. The identity of the single photoproduct (not isolated) was established as the naphthoxazole derivative from its mass spectra that shows a molecular ion of mass 245. In addition, retention time and mass spectra matching to that obtained in identical chromatographic conditions for the pure compound synthesized previously.[34] The formation of a single naphthoxazol derivative was also observed in the photolysis of compounds **2** and **3**.

In the presence of amines such as triethylamine (TEA) the consumption quantum yield increases depending on the amine concentration and the product distribution is more complex. A sequence of chromatograms was obtained upon photolysis of naphthoxazinone **2** in Ar-saturated benzene at various irradiation times. At short irradiation times, besides the signal with retention time 7.62 min, with a mass spectra corresponding to the nonphotolized naphthoxazinone **2**, only one photoproduct with retention time of 7.90 min could be observed. The spectrum of compound with retention time 7.90 min shows a molecular ion with *m*/*z* 275, two mass units larger than napthoxazinone **2**, indicating the formation of a dihydronaphthoxazinone derivative. The presence of this compound as the main photoreaction product at low conversion was corroborated by comparison with the mass spectrum and retention time of the CG-MS chromatogram measured for a genuine sample synthesized by catalytic hydrogenation of naphthoxazinone **2** and characterized by its ^{1}H NMR spectrum. At larger photolysis time (over 10 min), new peaks become visible in the chromatogram at retention time of 6.26 and 6.82 min. The signal appearing at 6.26 min shows a mass spectra with a molecular ion *m*/*z* equal to 245 and a fragmentation pattern corresponding to the oxazole derivative of naphthoxazinone **2**. In addition, the mass spectrum of the peak with retention time of 6.82 min that shows a molecular ion of *m*/*z* equal to 247. This last result is compatible with the formation of an oxazoline derivative that could be a product of photolysis of the dihydronaphthoxazinone (t_R = 7.90 min). The dihydronaphthoxazinone apparently is the primary photoproduct, which accumulates at the beginning of photolysis. In order to corroborate that the oxazoline derivative is the only product in the photolysis of the dihydronaphthoxazinone, a purified sample of the dihydronaphthoxazinone, was irradiated under Ar in the absence and the presence of TEA, employing identical experimental conditions than those for the photolysis of **2**. In both experiments the GC-MS chromatograms show a single photo-

(34) Saitz, C.; Rodríguez, H.; Márquez, A.; Cañete, A.; Jullian, C.; Zanocco, A. L. *Synthetic Commun.* **2001**, *31*, 135–140.

SCHEME 2

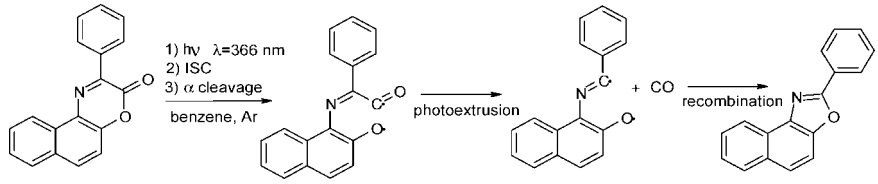

SCHEME 3

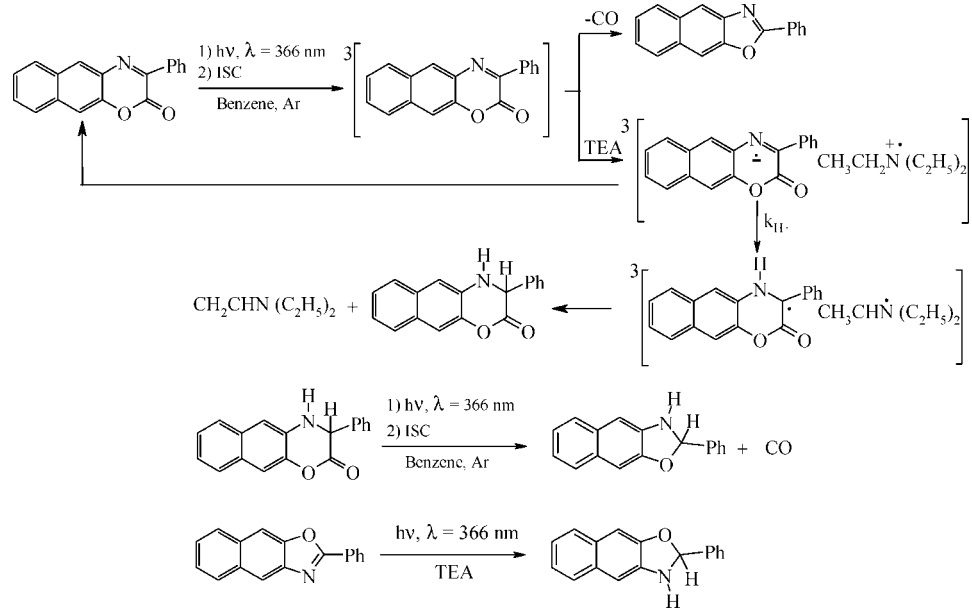

reaction product with $t_R = 6.82$ min and the same mass spectrum as the oxazoline derivative. In addition, the formation rate of the oxazoline derivative was independent of the presence of TEA. Photolysis of compounds **1** and **3** afforded the same product distribution observed for **2**, however in the photolysis of **1** and **3** the primary dihydronaphthoxazinone photoreaction product does not accumulate, indicating a smaller formation rate, a larger photoreaction rate of the dihydronaphthoxazinone to produce secondary products and/or an efficient back reaction of the primary intermediates produced in quenching by amine. The laser flash photolysis results allow us to disregard the first possibility, as the quenching rate constants are of the same order of magnitude for the three compounds but the photoconsumption quantum yields, at least 1 order of magnitude smaller for **1** and **3**, favor the last possibility.

The photoconsumption quantum yields, the rate constants for quenching of singlet and triplet states with TEA, and the product distribution allow us to explain the photochemical behavior of naphthoxazinone derivatives. A low photoconsumption quantum yield was determined in Ar-purged solutions for **1**, **2**, and **3** (in the absence of additives), being one order of magnitude larger for **2**. This result is compatible with the very low fluorescence quantum yield and the largest quantum yield of singlet oxygen formation observed for **2** and could be understood in terms of a more efficient intersystem crossing to the triplet excited states, probably promoted by $S_1(\pi,\pi^*)-T_n(n,\pi^*)$ spin−orbit coupling. In O_2 saturated and/or air equilibrated benzene solutions, they were stable up to 100 h of irradiation at 360 nm with a 150 W black ray lamp. This indicates that, in the absence of additives such as electron donors, the photoreactions of naphthoxazinone derivatives arise from the triplet excited state. In fact, the consumption quantum yields under argon in absence of additives, follow the same trend as the triplet yields. A simple photoextrusion mechanism involving a diradical intermediate is proposed to explain the formation of the naphthoxazole (Scheme 2).

Photoproduct formation through the triplet state is enhanced by the presence of TEA. As a typical example, when naphthoxazinone **2** was irradiated in benzene under Ar, the consumption quantum yield increased by a factor of 32 when 1.4×10^{-3} M of TEA was added, whereas no photoreaction was observed if the solution was saturated with O_2, even under extensive irradiation and in the presence of TEA. Also, quenching of singlet state did not exceed 8% at the TEA concentrations employed in these experiments.

We propose that the photoproducts observed upon photolysis of naphthoxazinone derivatives in the presence of TEA arise from electron-transfer from TEA to their triplet state (Scheme 3). The radical ion-pair formed can evolve to the starting products or a proton could be transferred from the amine radical cation to the naphthoxazinone radical anion to give a neutral radical pair. The primary stable product, the dihydro-naphthoxazinone, could thus be produced by disproportionation of this radical pair within the solvent cage. An analogous mechanism has been invoked to explain the formation of dihydroquinoxalin-2-ones by irradiation of 3-phenylquinoxalin-2-ones in the presence of amines.[35] The lower consumption quantum yield in **1** and **3** suggests that back electron transfer is more efficient in phenanthrene-like naphthoxazinones.

(35) De la Fuente, J. R.; Cañete, A.; Zanocco, A. L.; Saitz, C.; Jullian, C. *J. Org. Chem.* **2000**, *65*, 7949–7958.

Conclusions

The photophysics of the naphthoxazinone derivatives studied in this work is strongly dependent on the position of oxazolinone ring on the naphthalene moiety. Phenantrene-like naphthoxazinones exhibit fluorescence quantum yields higher than the less-aromatic anthracene-like homologous. In contrast, the latter show the strongest dependence of the emission maxima on the solvent polarity, indicating an important charge separation in the singlet excited state. Although all compounds are essentially photostable in the absence of additives, formation of a naphthoxazole derivative from the triplet excited-state is observed, albeit with very low quantum yield. The presence of electron donors such as amines enhances the photoconsumption quantum yield and changes the product distribution by opening a photoreaction mechanism mediated by electron transfer to the excited triplet state. Their photophysical properties and large photostability in air-equilibrated solutions suggest that naphthoxazinone derivatives could be valuable dyes for dye laser applications (**3**) as well as for singlet oxygen photosensitization (**2**).

Experimental Details

Materials. All solvents used in the syntheses and spectroscopic and kinetic measurements were of reagent grade, were of spectroscopic or HPLC quality, and were purified by the usual procedures when necessary.[36]

Chemical Synthesis. Naphthoxazinones-derivatives were obtained by employing a modification of the Moffet method.[37]

2-Phenyl-3H-naphtho[2,1-b][1,4]-oxazin-3-one (1).[34,38] Freshly distilled methyl benzoylformiate (2.09 mmol) and 1-aminonaphthol (2.75 mmol) in 20 mL of etanol/pyridine were heated at 110 °C by 1 h in a flask equipped with a reflux condenser and a magnetic stirrer. The precipitate obtained by cooling the mixture in ice−water bath was filtered and washed at least three times each with: water, diluted HCl, and water. Finally, the dry solid was recrystallized from acetonitrile to yield 0.75 g (80%) of the product as a yellow crystalline solid, mp 173.5−174.5 °C. Lit.[32] 174−175 °C. ^{1}H NMR ($CDCl_3$): δ 7.37 [d, 1H, J = 9.0 Hz]; 7.49 [m, 3H]; 7.53 [dd, 1H]; 7.65 [dd, 1H]; 7.83 [d, 1H, J = 8.1 Hz]; 7.90 [d, 1H, J = 9.0 Hz]; 8.46 [m, 2H]; 8.84 [d, 1H, J = 8.35 Hz]. ^{13}C NMR ($CDCl_3$): δ 116.1; 123.3; 126.8; 127.1; 128.5; 128.7; 128.8[d]; 129.8[d]; 130.9; 131.5; 131.7; 132.8; 134.9; 145.2; 148.8. IR (KBr): cm^{-1} 1725.7 (C═O); 1584.9 (*C*═N); Elem. anal. calcd %C: 79.11; %H: 4.06; %N: 5.13; exp. %C: 79.11; %H: 4.08; %N: 5.43.

Methods. The fluorescence quantum yields (Φ_F) were measured by the comparative method described by Eaton and Demas,[39,40] using quinine sulfate in 0.1 N sulfuric acid (Φ_F = 0.55)[41] or fluorescein in 0.1 N NaOH (Φ_F = 0,92)[41] as references. Optical densities of sample and reference solutions were set below 0.2 at the excitation wavelength, and the fluorescence spectra were corrected by using rhodamine G as reference. Sample quantum yield was evaluated by using eq 2:

$$\Phi_x = \left(\frac{Grad_x}{Grad_{\mathrm{Act}}}\right)\left(\frac{\eta_x^2}{\eta_{\mathrm{Act}}^2}\right)\Phi_{\mathrm{Act}} \qquad (2)$$

where $Grad_X$ and $Grad_{\mathrm{Act}}$ are the slope of integrated fluorescence vs absorbance plots for the sample and the actinometer, respectively, and η_x and η_{Act} are the refractive index of sample and actinometer, respectively. All measurements were carried out in nitrogen-purged solutions at (20 ± 0.5) °C.

Photoconsumption quantum yields under several experimental conditions were evaluated using the self-sensitized photooxygenation of 9,10-dimethylanthracene in air saturated Freon 113 (Φ = 0.566).[42,43] The photon flux, q/einstein s^{-1} was calculated according to eq 3:

$$q = \frac{\Delta A(324\ \mathrm{nm})V}{\Phi(\lambda)\varepsilon(324\ \mathrm{nm})tl} \qquad (3)$$

with t = irradiation time, V = volume of the solution, l = optical path length, $\Phi(\lambda)$ = photo-oxigenation quantum yield, and ε(324 nm) = molar absorption coefficient. Time-dependent naphthoxazinone photoconsumption was measured from its absorption spectra and/or by the decreasing of the peak area in the GC-NPD chromatogram. Additional experiments using the benzophenone/benzhydrol actinometer[44,45] were performed to confirm values in selected experiments. Not more than 20% of a difference between the two actinometers employed was observed for a given experiment.

The rate constant for quenching of the naphthoxazinone singlet state by a series of amines (^1k_q) was determined from a Stern−Volmer analysis of the amine effect on the naphthoxazinone steady-state fluorescence intensity using eq 4:

$$\frac{I^0}{I} = 1 + K_{\mathrm{SV}}[\mathrm{Q}] \qquad (4)$$

where I^0 and I are the areas under the fluorescence spectrum at zero and higher concentrations of the amine, respectively, and K_{SV} is the Stern−Volmer constant (= $^1k_q\,\tau^0_S$, where τ^0_S is the singlet lifetime at zero amine concentration).

Fluorescence lifetimes, τ^0_S, were measured by employing the phase demodulation method using fluorescein as reference (τ^0_S = 4.05 ns).[46,47] Phase shift and emission demodulation were employed to calculate τ^0_S according to eqs 5 and 6:

$$\tau_p = \omega^{-1}\tan\phi \qquad (5)$$

$$\tau_m = \omega^{-1}\left(\frac{1}{m^2} - 1\right)^{1/2} \qquad (6)$$

where τ_p is the phase lifetime, τ_m the demodulation lifetime, ω the circular frequency of the incident light, ϕ the phase angle displacement, and m is the demodulation factor. Measured values gave $\tau_p = \tau_m = \tau^0_S$, indicating monoexponential fluorescence decays.

Rate constants for quenching of the triplet state by TEA were determined examining the effect of this amine on the rate of triplet decay. In the presence of a quencher, the observed pseudofirst order rate constant for triplet decay, $^3k_{\mathrm{obs}}$, increases linearly as shown in eq 7:

$$^3k_{\mathrm{obs}} = 1/\tau_T = 1/\tau^0_T + {}^3k_q^{\mathrm{TEA}}[\mathrm{TEA}] \qquad (7)$$

Values of $^3k_q^{\mathrm{TEA}}$ were deduced from the slope of the linear plot of $^3k_{\mathrm{obs}}$ vs the concentration of TEA.

(36) Wiberg, K. B. *Laboratory technique in organic chemistry*; McGraw-Hill: New York, 1960.
(37) Mofett, R. B. *J. Med. Chem.* **1966**, *9*, 475–478.
(38) Márquez, A.; Saitz, C.; Cañete, A.; Rodríguez, H.; Jullian, C. *Mag. Reson. Chem.* **1998**, *36*, 449–453.
(39) Eaton, D. F. *Pure Appl. Chem.* **1988**, *60*, 1107–1114.
(40) Demas, J. N.; Crosby, G. A. *J. Phys. Chem.* **1971**, *75*, 991–1024.
(41) Heller, C. A.; Henry, R. A.; McLaughlin, B. A.; Bliss, D. E. *J. Chem. Eng. Data* **1974**, *19*, 214–219.
(42) Adick, H.-J.; Schmidt, R.; Brauer, H.-D. J. *Photochem. Photobiol. A: Chem.* **1988**, *45*, 89–96.
(43) Kuhn, H. J.; Braslavsky, S. E.; Schmidt, R. *Pure Appl. Chem.* **2004**, *76*, 2105–2146.
(44) Borderie, B.; Lavabre, D.; Levy, G. *J. Photochem. Photobiol. A: Chem.* **1991**, *56*, 13–23.
(45) Murov, S. L. *Handbook of Photochemistry*, 2nd ed.; Marcel Dekker, New York, 1993; Sect. 13, p 307.
(46) Nunnally, B. K.; He, H.; Li, L.-C.; Tucker, S. A.; McGown, L. B. *Anal. Chem.* **1997**, *69*, 2392–2397.
(47) Pant, S.; Tripathi, H. B.; Pant, D. D. *J. Photochem. Photobiol. A: Chem.* **1994**, *81*, 7–11.

Acknowledgment. Financial support from FONDECYT (grants 1050796 and 7060251) is gratefully acknowledged.

Supporting Information Available: General experimental methods, experimental synthetic procedures, spectroscopic and analytical data for naphthoxazinone derivatives **2** and **3** and the corresponding dihydronaphthoxazinone photoproducts, ^{1}H NMR, ^{13}C NMR, and mass spectra. Absolute energies, lowest-energy Franck−Condon transition, Cartesian coordinates, Mulliken charge distribution, and HOMO/ LUMO localization of naphthoxazinone derivatives **1**, **2**, and **3**. This material is available free of charge via the Internet at http://pubs.acs.org.

JO800039R